

## Tuning the emission wavelength of Si nanocrystals in SiO<sub>2</sub> by oxidation

M. L. Brongersma<sup>a)</sup> and A. Polman

*FOM Institute for Atomic and Molecular Physics, Kruislaan 407, 1098 SJ Amsterdam, The Netherlands*

K. S. Min, E. Boer, T. Tambo, and H. A. Atwater

*Thomas J. Watson Laboratory of Applied Physics, California Institute of Technology, Pasadena, California 91125*

(Received 6 October 1997; accepted for publication 17 March 1998)

Si nanocrystals (diameter 2–5 nm) were formed by 35 keV Si<sup>+</sup> implantation at a fluence of  $6 \times 10^{16}$  Si/cm<sup>2</sup> into a 100 nm thick thermally grown SiO<sub>2</sub> film on Si (100), followed by thermal annealing at 1100 °C for 10 min. The nanocrystals show a broad photoluminescence spectrum, peaking at 880 nm, attributed to the recombination of quantum confined excitons. Rutherford backscattering spectrometry and transmission electron microscopy show that annealing these samples in flowing O<sub>2</sub> at 1000 °C for times up to 30 min results in oxidation of the Si nanocrystals, first close to the SiO<sub>2</sub> film surface and later at greater depths. Upon oxidation for 30 min the photoluminescence peak wavelength blueshifts by more than 200 nm. This blueshift is attributed to a quantum size effect in which a reduction of the average nanocrystal size leads to emission at shorter wavelengths. The room temperature luminescence lifetime measured at 700 nm increases from 12 μs for the unoxidized film to 43 μs for the film that was oxidized for 29 min. © 1998 American Institute of Physics. [S0003-6951(98)03220-3]

The recent discovery of visible light emission from nanocrystalline group IV materials has stimulated considerable experimental effort to understand its origin and utilize it to fabricate Si-based optoelectronic devices.<sup>1–4</sup> The process of making Si nanocrystals by Si ion implantation into thermal SiO<sub>2</sub> films on Si, followed by precipitation,<sup>5–7</sup> is fully compatible with standard integrated circuit technology and the SiO<sub>2</sub> matrix is a robust host that provides good passivation for the Si nanocrystals. Previously, we have demonstrated that SiO<sub>2</sub> films containing Si nanocrystals made by ion implantation show photoluminescence in the visible and near-infrared that can be attributed to two distinct sources. One luminescence feature is related to ion irradiation induced defects in the SiO<sub>2</sub> matrix and can be quenched by introducing H or D into the film.<sup>6</sup> The other has been attributed to radiative recombination of quantum-confined excitons in the Si nanocrystals. We have also shown that the nanocrystal luminescence intensity can be increased by as much as a factor of 10 by annealing a deuterated sample at 400 °C, which is attributed to the passivation of dangling bonds at the nanocrystal/SiO<sub>2</sub> interface.<sup>6</sup> Previously, it has been shown that the luminescence from Si nanocrystals in SiO<sub>2</sub> can be continuously redshifted by thermal annealing, due to an increase in the crystallite size.<sup>8</sup>

In this letter, we demonstrate that the photoluminescence (PL) peak wavelength from Si nanocrystals embedded in an SiO<sub>2</sub> film can be blueshifted by more than 200 nm by thermal oxidation at 1000 °C. Transmission electron microscopy (TEM) and Rutherford backscattering spectrometry (RBS) measurements show the oxidation of Si particles starts near the surface of the SiO<sub>2</sub> film and as time progresses, an oxidation front moves deeper into the film. The PL blueshift is attributed to a decrease in the average nanocrystal size as the

oxidation progresses, in agreement with quantum confinement theory.

SiO<sub>2</sub> films (100 nm thick) grown by wet thermal oxidation of lightly *p*-doped (100) Si wafers were implanted at room temperature with 35 keV Si<sup>+</sup> at a fluence of  $6 \times 10^{16}$ /cm<sup>2</sup>, resulting in a Si concentration at the peak of the implantation profile of 44 at. %, as determined by RBS. These samples were subsequently annealed at 1100 °C for 10 min in vacuum at a base pressure below  $3 \times 10^{-7}$  mbar to induce nucleation and growth of Si nanocrystallites.<sup>5–7</sup> Oxidation was performed in flowing O<sub>2</sub> (flow rate=47 sccm) at 1000 °C and at 1 atm for times ranging from 0 to 30 min. Finally, 600 eV deuterium was introduced into all samples to quench the defect related luminescence by means of implantation using a Kauffman ion source,<sup>6</sup> and the Si nanocrystal luminescence was optimized by a subsequent anneal at 400 °C for 10 min. Cross-sectional bright-field TEM images were taken to determine their presence and distribution in the oxide film. RBS was used to determine the Si depth profile using a 2 MeV He<sup>+</sup> beam at a scattering angle of 93° and an angle of 3° between the sample normal and the incident He<sup>+</sup> beam. The depth resolution was 10 nm. Room temperature (RT) PL spectra were taken using the 457.9 nm line of an Ar ion laser at a pump power density of 10 mW/mm<sup>2</sup> and detected by a grating spectrometer in combination with a thermoelectrically cooled Si charge coupled device (CCD) detector array. All spectra were corrected for the system response. PL lifetime measurements were made after pumping to steady state with a power density of 0.2 mW/mm<sup>2</sup>. The pump light was chopped with an acousto-optic modulator and the lifetime traces were taken with a GaAs photomultiplier in combination with a multichannel photon counting system. The time resolution of the setup was 400 ns.

Figure 1(a) shows a bright-field cross-sectional TEM image of the implanted SiO<sub>2</sub> film after annealing in vacuum at 1100 °C. The image was taken at a slightly defocused con-

<sup>a)</sup>Electronic mail: Brongersma@amolf.nl; <http://www.amolf.nl/departments/optoelec>

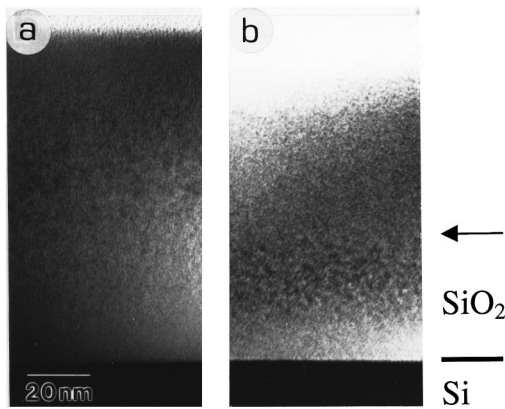


FIG. 1. Cross-sectional bright-field TEM images of (a) a 100 nm thick  $\text{SiO}_2$  film on (100) Si implanted with 35 keV  $\text{Si}^+$  to a fluence of  $6 \times 10^{16} \text{ Si/cm}^2$  and annealed at 1100 °C for 10 min. (b) The same sample after annealing in  $\text{O}_2$  at 1000 °C for 15 min. The arrow indicates the location of the oxidation front.

dition to enhance the contrast. Despite the weak Z contrast between Si and  $\text{SiO}_2$ , it shows a dense array of Si particles in the size range of 2–5 nm distributed throughout the whole oxide film. The nanocrystals in the center of the  $\text{SiO}_2$  film are slightly larger than those near the surface and near the Si substrate. This is attributed to the fact that implantation produces a Gaussian shaped Si concentration depth profile with a peak excess concentration of Si in the center of the oxide film. We have shown before, using high resolution TEM, that these Si particles are single crystalline.<sup>6</sup>

Figure 1(b) shows a cross-sectional bright-field TEM image taken from the same sample after receiving an oxidation step at 1000 °C for 15 min. In a  $\sim 60$  nm thick surface region all nanocrystals have oxidized away (at least to a size smaller than the detection limit of 1.5 nm), while a  $\sim 40$  nm thick region near the interface with the Si substrate clearly shows the presence of nanocrystals.

Figure 2 shows the RBS spectrum of the implanted and annealed film before oxidation (indicated by a “0”). The surface channel for Si in  $\text{SiO}_2$  is indicated by an arrow. It shows the Si depth profile with a peak concentration of 44

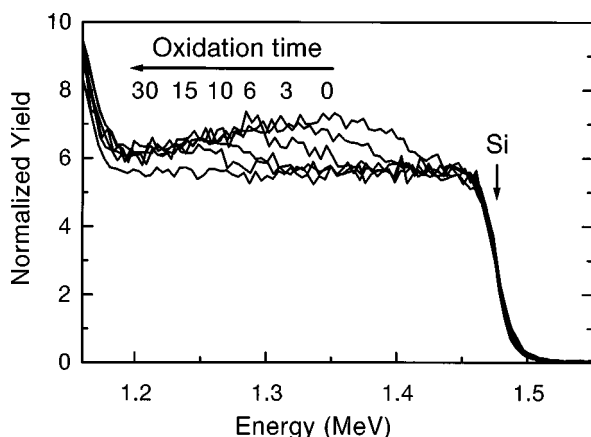


FIG. 2. RBS spectra of 100 nm thick  $\text{SiO}_2$  films on (100) Si implanted with  $6 \times 10^{16} \text{ Si/cm}^2$ , annealed at 1100 °C for 10 min, and subsequently oxidized at 1000 °C for 0, 3, 6, 10, 15, and 30 min. The oxidation times are indicated at the peak of the Si depth profile of the corresponding RBS spectrum. The horizontal arrow indicates the direction in which the oxidation front moves. The Si surface channel is also indicated by an arrow.

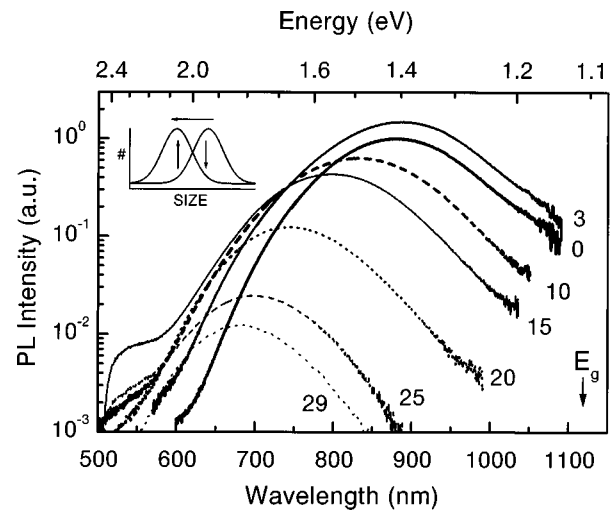


FIG. 3. Room temperature PL spectra plotted on a logarithmic intensity scale, measured on 100 nm thick  $\text{SiO}_2$  films containing Si nanocrystals, that were oxidized for 0, 3, 10, 15, 20, 25, and 29 min at 1000 °C. For each spectrum, the corresponding oxidation time is indicated. The band-gap wavelength of bulk Si is indicated by an arrow. The inset schematically shows the change in the nanocrystal size distribution upon oxidation.

at. % at roughly 40 nm below the surface. Figure 2 also shows the RBS spectra taken after annealing in flowing oxygen at 1000 °C for 3, 6, 10, 15, and 30 min. It can be clearly seen that the oxidation of Si nanocrystals starts at the surface and as time progresses, the oxidation front moves deeper into the film. After 3 min the oxidation front has reached a depth of 50 nm and the Si concentration near the surface is approximately 33 at. %, the Si concentration in stoichiometric  $\text{SiO}_2$ . Upon further oxidation the oxidation front moves slower but steadily deeper into the film and after 30 min the whole film is reconverted into  $\text{SiO}_2$ . It should be noted that the oxidation front is much wider than the RBS depth resolution ( $\approx 10$  nm), indicating that a relatively wide cluster doped region is oxidizing at the same time.

Figure 3 shows room temperature PL spectra of the films taken before and after oxidation for 3, 10, 15, 20, 25, and 29 min, plotted on a logarithmic intensity scale. The PL spectrum of the unoxidized sample (“0”) shows a broad peak centered around 880 nm, in agreement with the estimated recombination energy for quantum-confined excitons in a  $\approx 3$  nm diam Si nanocrystal,<sup>9</sup> corresponding to about 700 atoms per crystal. The width of the emission band is attributed to a wide distribution in nanocrystal sizes.<sup>4,9</sup> As can be seen in Fig. 3(a), the intensity increases over the whole wavelength region by a factor of  $\approx 1.5$  after 3 min oxidation, and then decreases for longer oxidation times. Furthermore, oxidation leads to a continuous blueshift of the spectrum. After oxidation for 29 min, the emission peaks at 680 nm. Taking into account the tails of the spectra, this oxidation technique can be used to tune the luminescence from 500 nm (green) all the way to the band gap of bulk Si at 1.11  $\mu\text{m}$ . An emission wavelength of 500 nm corresponds to a crystal diameter of  $\approx 1$  nm ( $\approx 26$  atoms).<sup>9</sup>

In the case of a system of noninteracting Si nanocrystals, the luminescence intensity at each wavelength is determined by the number density of Si nanocrystals, their absorption cross section, and their luminescence efficiency. Nanocrystals luminescing at different wavelengths will have different

absorption cross sections as the absorption cross section depends on the size. However, at a fixed wavelength, changes in the PL intensity can be translated directly into a change in the number density of luminescing nanocrystals of a particular size. Since the total number of nanocrystals decreases upon oxidation, the initial intensity increase observed after 3 min oxidation must be attributed to an increase in the luminescence efficiency. It is known that Si nanocrystals made by thermal annealing of a Si-rich oxide have a suboxide layer between the nanocrystal and the SiO<sub>2</sub> matrix<sup>10</sup> that could give rise to nonradiative decay channels for quantum-confined excitons. Possibly, the oxidation treatment can remove these nonradiative decay channels (and thus increase the luminescence efficiency) by making the nanocrystal surroundings more stoichiometric. The RBS measurements show that after 3 min oxidation, half of the Si profile is affected by the oxidation, resulting in possible changes in the luminescence efficiency for all crystallite sizes, as observed. The overall decrease in the intensity observed for longer oxidation times is attributed to three effects, namely: (1) the number density of Si nanocrystals decreases, (2) the absorption cross section decreases for optical excitation with decreasing nanocrystal size,<sup>9</sup> (3) the oxidation process may yield nanocrystals that do not luminesce.

According to quantum confinement theories the band gap of a Si nanocrystal increases with decreasing nanocrystal size.<sup>9</sup> Comparing the luminescence spectra for 3, 10, and 15 min, it can be seen that for a fixed wavelength above 740 nm the intensity *decreases* as the oxidation time increases, while it *increases* at shorter wavelengths. This behavior can be explained in terms of a shift of the nanocrystal size distribution to smaller sizes due to the oxidation process, as indicated schematically in the inset of Fig. 3. The number density of nanocrystals emitting at shorter wavelengths than 0.74  $\mu\text{m}$  grows due to the oxidation of larger nanocrystals emitting at longer wavelengths. After oxidation for 15 min, when nearly all the large nanocrystals in the center of the oxide film have been oxidized (see RBS and TEM), the intensity at the long wavelength side of the PL spectrum ( $>950$  nm) has decreased by more than an order of magnitude. For longer oxidation times (20, 25, 29 min) the PL spectrum continues to shift towards the blue, indicating a further decrease in the average size of the luminescing nanocrystals. Eventually, after oxidation for 30 min all nanocrystals have been oxidized and no PL is observed.

Figure 4 shows normalized RT luminescence decay traces taken at 700 nm from some of the samples that were shown in Fig. 3. A stretched exponential function:  $I(t) = I_0 \exp(-t/\tau)^\beta$ , was fitted to the data, in which  $\tau$  is an effective decay time, and  $\beta$  a constant between 0 and 1. For the unoxidized sample we find  $\tau = 12 \mu\text{s}$  and  $\beta = 0.63$ . Upon oxidation  $\tau$  and  $\beta$  monotonously increase up to values of  $\tau = 43 \mu\text{s}$  and  $\beta = 0.79$  for 29 min oxidation.

A lifetime on the order of tens of  $\mu\text{s}$  is indicative of the fact that the Si nanocrystals behave as an indirect band-gap semiconductor, as is expected for nanocrystals luminescing at this wavelength.<sup>4,9</sup> Stretched exponential decay of the luminescence is commonly observed for Si nanocrystals in an oxide matrix, porous Si, and other materials that are disordered or inhomogeneous on the microscopic scale.<sup>2-4</sup> In the

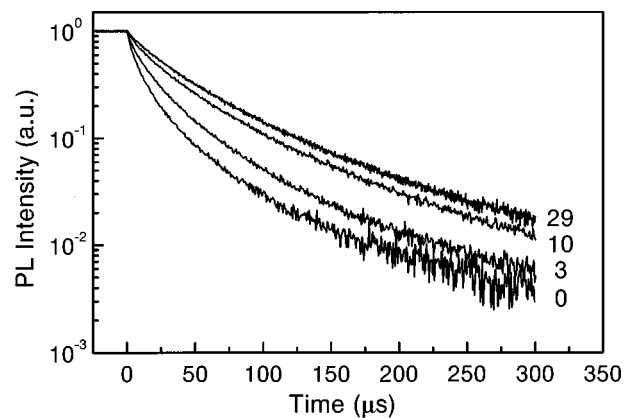


FIG. 4. Normalized RT luminescence decay traces taken at 700 nm from SiO<sub>2</sub> films containing Si nanocrystals that were oxidized for 0, 3, 10, and 29 min at 1000 °C. For each decay trace the corresponding oxidation time is indicated.

ideal case of noninteracting nanocrystals that can only decay radiatively, a single exponential decay is expected, i.e.,  $\beta = 1$ . The experimental fact that  $\beta < 1$  demonstrates that interaction between neighboring nanocrystallites, or between nanocrystallites and defect states may play an important role in the PL behavior. The increase in both  $\tau$  and  $\beta$  then shows that upon oxidation the nanocrystals emitting at 700 nm more and more approach the ideal case of a collection of noninteracting radiatively decaying nanocrystals.

In conclusion, we demonstrate that thermal oxidation of SiO<sub>2</sub> films containing Si nanocrystals results in a substantial blueshift of the PL spectrum due to a continuous decrease in the average nanocrystals size. TEM and RBS show that the oxidation of the Si nanocrystals starts close to the surface, followed by oxidation of nanocrystals located at a greater depth. The RT luminescence lifetime measured at 700 nm was on the order of 10  $\mu\text{s}$ , indicative of the fact that the Si nanocrystals behave as an indirect band-gap material. The decay traces become more single exponential upon oxidation, which is attributed to a decrease in the interaction of the nanocrystals with their surroundings.

The work at FOM was financially supported by NWO, STW, and the SCOOP program of the European Union. Further support was obtained from the U.S. Department of Energy under Grant No. DE-FG03-89ER45395 and the NATO Ministry for Scientific Affairs.

- <sup>1</sup>L. T. Canham, Appl. Phys. Lett. **57**, 1046 (1990).
- <sup>2</sup>R. W. Collins, P. M. Fauchet, I. Shimizu, J. C. Vial, T. Shimada, and A. P. Alivisatos, Mater. Res. Soc. Symp. Proc. **452**, (1996).
- <sup>3</sup>J. C. Vial and J. Derrien, Porous Si Science and Technology (Springer, Berlin, 1995).
- <sup>4</sup>Y. Kanemitsu, Phys. Rep. **263**, 1 (1995).
- <sup>5</sup>T. Shimizu-Iwayama, M. Ohshima, T. Niimi, S. Nakao, K. Saitoh, T. Fujita, and N. Itoh, J. Phys.: Condens. Matter **5**, L375 (1993).
- <sup>6</sup>K. S. Min, K. V. Shcheglov, C. M. Yang, H. A. Atwater, M. L. Brongersma, and A. Polman, Appl. Phys. Lett. **69**, 2033 (1996).
- <sup>7</sup>T. Komoda, J. Kelly, F. Cristiano, A. Nejim, P. L. F. Hemment, K. P. Homewood, R. Gwilliam, J. E. Mynard, and B. J. Sealy, Nucl. Instrum. Methods Phys. Res. B **96**, 387 (1995).
- <sup>8</sup>T. Fischer, V. Petrova-Koch, K. Scheglov, M. S. Brandt, F. Koch, and V. Lehmann, Thin Solid Films **276**, 100 (1996).
- <sup>9</sup>M. Hybertsen, Phys. Rev. Lett. **72**, 1514 (1994).
- <sup>10</sup>P. Brüesch, Th. Stockmeier, F. Stucki, and P. A. Buffat, J. Appl. Phys. **73**, 7666 (1993).